The Astrophysical Journal, 687: 623–634, 2008 November 1

ENERGY-DEPENDENT CHARGE STATES AND THEIR CONNECTION WITH ION ABUNDANCES IN IMPULSIVE SOLAR ENERGETIC PARTICLE EVENTS

R. DiFabio,[1] Z. Guo,[1] E. Möbius,[1] B. Klecker,[2] H. Kucharek,[1] G. M. Mason,[3] and M. Popecki[1]

Received 2006 May 16; accepted 2008 July 11

ABSTRACT

Impulsive solar energetic particle (SEP) events show substantial enhancements of heavy ions and ^{3}He over the composition in the Sun's atmosphere. Mass per charge dependent acceleration mechanisms have been proposed to account for this preferential acceleration. However, a problem emerged for all the preferential acceleration models with the measurement of ionization states near 1 MeV nucleon^{-1}, which showed that ions from C to Mg are fully stripped, a challenge that had been recognized early on. Since all models relied on differences in the charge-to-mass ratio to enable preferential acceleration, the proposed mechanisms were incompatible with this observation. Recent observations of the ionic charge states at lower energies have revealed a dependence on energy, with the charge states decreasing for lower energy ions. This raises the possibility that the low-energy charge states reflect the plasma conditions at the acceleration site, while the high-energy charge states are due to stripping low in the solar corona. In a survey of impulsive events we show that the increase of the Fe charge states with energy is highly significant for the sample of events and thus most likely a general feature of impulsive events. To see whether there is a connection between the enhancements and charge states, we extended the *ACE* SEPICA charge-state observations to lower energies and combined them with the ion fluxes from *ACE* ULEIS for impulsive events observed between 1997 and 2000. We find a positive correlation between the abundance ratios and the charge states at low energy, while the charge states at the highest energy do not demonstrate such dependence. This supports the idea that the higher mass particles are preferentially accelerated before being stripped.

Subject headings: acceleration of particles — Sun: particle emission

1. INTRODUCTION

Solar energetic particle (SEP) events are usually grouped into two categories: gradual and impulsive (Reames 1990). Gradual events have a typical duration of several days and are associated with coronal mass ejections (CMEs; Sheeley et al. 1975, 1983; Kahler 1977). The ions in gradual events are often associated with shocks that accompany CMEs. Impulsive SEPs typically last only a few hours and have been observed to be highly dispersive (Mazur et al. 2000a, 2000b). These events are associated with impulsive flares (e.g., Reames et al. 1988) and have substantial enhancements of the isotope ^{3}He (Hsieh & Simpson 1970; Dietrich 1973; Garrard et al. 1973) and heavy ions (Mg, Ne, Fe) compared to the composition of the solar corona (Mason et al. 1986, 1994; Dwyer et al. 2001). Recently, it has been shown that these heavy ion overabundances extend to ultraheavy ions (up to 200 AMU), with values that exceed those for Fe by 1–2 orders of magnitude (Reames 2000; Mason et al. 2004; Reames & Ng 2004). Sometimes impulsive events have unusual enhancement patterns that favor N and S (Mason et al. 2002), but most often the enhancements increase smoothly with particle mass.

A number of different plasma wave resonant mechanisms have been used to explain the preferential acceleration of ^{3}He (Temerin & Roth 1992; Fisk 1978; Varvoglis & Papadopoulos 1983; Zhang 1995; Ibragimov & Kocharov 1978; Miller & Vinas 1993; Liu et al. 2006). The heavy ion enrichments have also been modeled using plasma waves, although generally of a different kind than those that operate on the ^{3}He (e.g., Miller 1998; Zhang & Wang 2003). In all cases, the preferential acceleration mechanisms depend on the ionic mass per charge (M/Q), so the charge state of the ions plays a key role in the enhancements.

However, the first observations of charge states in impulsive events revealed very high values with $Q_{\rm Fe} \approx 20+$, with the ions from C to Si being fully stripped (Klecker et al. 1984; Luhn et al. 1987), in the energy range 0.55–3.0 MeV nucleon^{-1} for Si and 0.34–1.8 MeV nucleon^{-1} for Fe. It was thought that these high charge states were a result of very high temperatures in the source region. Because fully stripped ions from C to Si have identical M/Q values, these observations were incompatible with all of the proposed selective acceleration models. As a possible resolution of this problem, Reames et al. (1994) suggested selective acceleration of heavy ions out of a $(3–5) \times 10^6$ K plasma, inferred from the observed abundance ratios and subsequent increase of the charge states. Recent observations of the charge states using advanced instruments on board the *Advanced Composition Explorer* (*ACE*) and *Solar and Heliospheric Observatory* (*SOHO*) have extended the charge-state measurements to lower energies and found that the ionization states decreased—that is, the ions were no longer fully stripped (Möbius et al. 2003; Klecker et al. 2006). These observations of energy-dependent charge states could point to a solution of the problem between the higher energy charge-state observations and the current selective acceleration models.

Faced with the incompatibility between the fully stripped ions and enhanced abundances, a number of authors explored the possibility that the ionization states were caused by stripping after acceleration and therefore after the presumed preferential acceleration of the ^{3}He and heavy ions (Reames et al. 1999; Barghouty & Mewaldt 1999; Kocharov et al. 2000, 2001; Stovpyuk & Ostryakov 2001). Since the low-energy ions have a much lower velocity than coronal electrons, their ionization states depend only on the local plasma temperature. Therefore, the low-energy charge states will reflect the plasma conditions at the acceleration site. As

[1] Space Science Center and Department of Physics, University of New Hampshire, Durham, NH 03824.
[2] Max-Planck-Institut für extraterrestrische Physik, Garching, Germany.
[3] Johns Hopkins University/Applied Physics Laboratory, Laurel, MD 20723.

the velocity of the accelerated ions approaches and then exceeds the thermal velocity of the electrons, accelerated ions will be stripped of more electrons depending on their kinetic energy. As a consequence, the charge states will depend on energy.

Using early observations with *ACE*, Möbius et al. (2000) and Leske et al. (2003) also found that the charge states correlate with the abundance ratios for samples that contained impulsive and gradual events, which could have pointed to the mixture of ions from different event types or to a physical mechanism. With the newly established energy dependence of the charge states, it is possible that this correlation is dominated by the charge states at low energies where the acceleration starts out of an ambient plasma population.

In order to explore these issues in greater detail, we measured charge states and abundance ratios for a number of impulsive events from 1997 to 2000. In particular, we have extended the charge-state measurements with *ACE* SEPICA for a subset of the impulsive events to lower energies than those in our previous work (Möbius et al. 2003) to more fully examine the energy dependence. We find that the mean charge states of Fe for 0.18–0.43 MeV nucleon^{-1} (used as the survey energy range for SEPICA data) and heavy ion enhancements show a significant correlation. When separated by energy this trend appears to persist for the charge states at low energies, but not at high energies.

2. INSTRUMENTATION AND DATA ANALYSIS

The study reported here was carried out with instruments on the *Advanced Composition Explorer* spacecraft, which was launched in 1997 August into a halo orbit around the Lagrangian point L1 between the Earth and the Sun (Stone et al. 1998). For our studies we have used the Solar Energetic Particle Ionic Charge Analyzer (SEPICA; Möbius et al. 1998) to determine the charge states and the Ultra-Low Energy Isotope Spectrometer (ULEIS; Mason et al. 1998) to evaluate the abundances of energetic ions with energies of a few hundred keV nucleon^{-1} in impulsive solar energetic particle events.

SEPICA measures ion charge, energy, and ionization state by deflecting the ions with an electrostatic collimator that is followed by a position-sensing proportional counter to measure ΔE and the impact position of the ion. Finally, a solid-state detector measures the residual energy $E_{\rm SSD}$. Figure 1 shows a plot of ΔE vs. residual energy from SEPICA, where it can be seen that each ion species (with nuclear charge Z) leaves a unique track, which is not affected by the ionic charge state Q of the ions. Since the electrostatic deflector-collimator combination determines the E/Q of the ions, the charge state of each incoming ion can be calculated after the total energy E is evaluated as the combination of ΔE, $E_{\rm SSD}$, and calibrated energy losses in the counter windows and the solid state detector. A charge-state distribution is compiled from the individual ions over selected energy ranges along one of the tracks for the entire energetic particle event. From these distributions we determine the mean charge state as well as the standard deviation.

When ion energies fall below ~1 MeV nucleon^{-1} in the proportional counter, their charge states Q fall well below the nuclear charge Z and become comparable for different ion species, thus leading to indistinguishable energy loss and tracks that merge together, as can be seen in Figure 1. This effect limited our earlier studies to energies above ~0.18 MeV nucleon^{-1} for Fe. However, as can be seen in Figure 1, the Fe track crosses over the oxygen track and reemerges at even lower energies. This region between O and C is labeled "extended range" in Figure 1. Because N, which is found in this region between C and O, is usually less abundant than O by approximately 1 order of magnitude and

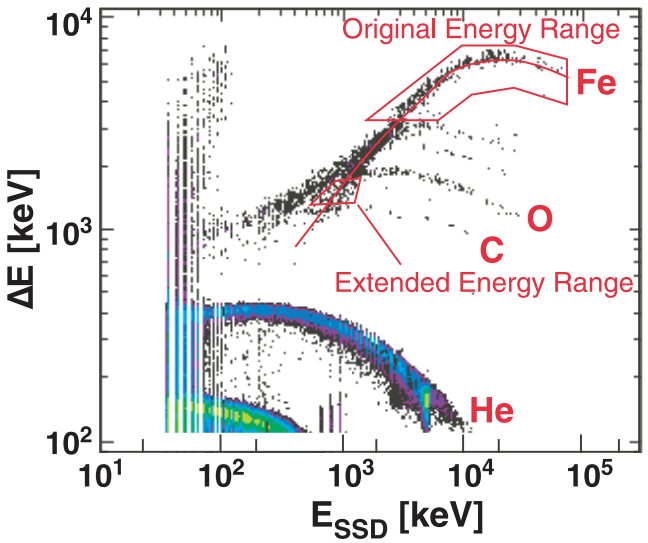

FIG. 1.—Energy loss (ΔE) in the proportional counter vs. energy ($E_{\rm SSD}$) measured in the SSD. Each ion species leaves a unique track. At energies below 0.18 MeV nucleon^{-1} the tracks for different ion species start to merge. However, the Fe track crosses over the O track and then re-emerges with only small interference from N. Red labeled boxes show the original Fe energy range and the extended range introduced in this work.

impulsive events have substantial overabundance of Fe, it is possible to obtain an accurate estimate of the Fe charge states at this low-energy range (0.062–0.11 MeV nucleon^{-1}), after subtracting the small N abundance (typically 10%–20%) that is in the same region as the Fe track. A more detailed description of this procedure can be found in an Appendix to this paper.

The abundance ratios are provided by ULEIS, which determines the kinetic energy per nucleon of the incoming ions by measuring the time of flight (TOF). Their residual kinetic energy is then measured using solid state detectors. The combination of the two measurements provides the mass of the ions and thus the ion species. We obtained the ULEIS heavy ion fluxes for the energy range 0.24 ± 0.08 MeV nucleon^{-1} and calculated the abundance ratios for Fe/O, Mg/O, Ne/O, with uncertainties determined from the number of counts of each species. The ^{3}He/^{4}He ratio was calculated over the energy range 0.39 ± 0.07 MeV nucleon^{-1}, which is the lowest energy interval for which there are good counting statistics.

For our study, we surveyed the temporal characteristics, composition, and ionic charge states of impulsive events during the entire time when SEPICA was fully operational from turn-on in 1997 September through late 2000, based on the temporal characteristics, composition, and ionic charge states. The proportional counters of SEPICA were not functional for several time periods (expressed as day of year [DOY]), i.e., 1998 DOY 13–57 and DOY 313 through 1999 DOY 166 because of problems with the gas pressure control valves. In addition, SEPICA was disabled during resets of the data processing unit, for example, 1998 DOY 160–166, 188–197, and 235–257. During these times no SEPICA data were available. Table 1 lists all the events in this survey with their integration times. It also shows the mean charge state of Fe in the SEPICA survey energy range of 0.18–0.43 MeV nucleon^{-1} as well as the ^{3}He/^{4}He and Fe/O ratios as obtained with ULEIS. It should be noted that the Fe charge states used here are based on SEPICA data with an updated calibration, correcting a known nonlinearity in the determination of the deflection when compared with results shown during the initial phase of the *ACE* mission (see, e.g., Möbius et al. 2002).

TABLE 1
IMPULSIVE EVENTS USED IN THIS STUDY

EVENT NUMBER	YEAR	TIME PERIOD (DOY:hr:min)	0.18–0.43 MeV nucleon^{-1}		0.39 MeV nucleon^{-1}		0.24 MeV nucleon^{-1}		SELECTION		
			Q_{Fe}	σ	^{3}He/^{4}He	σ	Fe/O	σ	INJECTION	$\Delta Q > 2.5$	$p < 0.1$
01	1998	136:00:00–137:00:00	16.92	0.68	0.01	0.002	4.15	0.356	s	1.5	0.543
02*	1998	149:18:00–151:00:00	17.35	0.69	0.05	0.003	0.47	0.025		3.7	0.029
03	1998	225:03:07–227:12:00	17.24	0.86	0.12	0.008	1.02	0.087		5.8	0.008
04	1998	227:12:00–228:08:52	16.66	1.02	0.13	0.018	0.65	0.065	s	0.9	0.643
05	1998	229:01:55–229:06:00	16.71	2.41	0.12	0.058	1.09	0.196	s	...	
06	1998	229:06:00–230:07:12	16.29	0.76	0.10	0.010	0.86	0.053	m	1.3	0.423
07	1998	230:07:12–231:00:00	17.51	1.07	5.09	0.359	1.81	0.187	s	0.3	0.942
08	1998	249:12:00–251:12:00	18.29	0.79	0.19	0.012	1.93	0.132		2.7	0.069
09*	1998	252:00:29–253:23:45	17.53	0.61	0.22	0.007	1.30	0.047	s	4.2	0.001
10*	1998	269:12:02–270:09:00	15.35	0.51	0.03	0.002	0.50	0.012		5.1	0.000
11*	1998	270:09:00–271:12:00	16.51	0.51	0.11	0.003	1.25	0.023	m	2.7	0.001
12*	1999	180:00:43–181:12:51	16.62	0.81	0.028	0.004	0.39	0.026	s	4.5	0.012
13*	1999	181:12:51–182:23:45	16.93	0.58	0.025	0.002	1.51	0.046	s	4.6	0.000
14*	1999	184:21:36–186:06:00	14.9	0.61	0.05	0.003	0.34	0.014	m	4.3	0.002
15*	1999	201:02:19–202:22:19	16.53	0.61	0.32	0.011	1.55	0.069	m	3.7	0.004
16	1999	207:00:00–207:21:30	17.58	1.06	0.87	0.072	0.65	0.059	s	4.8	0.029
17	1999	219:19:55–220:12:00	16.04	0.86	0.58	0.037	0.91	0.080	s	4.6	0.005
18	2000	6:06:00–7:00:00	15.54	1.56	43.56	7.349	1.48	0.179	s	3.3	0.363
19	2000	17:03:00–18:12:00	17.9	2.18	15.69	1.725	1.31	0.225	s	...	
20	2000	18:18:00–19:04:48	18.88	1.49	0.06	0.004	0.88	0.115	s	5.8	0.079
21	2000	60:00:00–61:18:00	15.24	1.54	0.62	0.038	1.06	0.088	m	3.1	0.373
22	2000	93:00:00–94:00:00	17.61	0.77	0.15	0.012	1.02	0.057	s	4.2	0.023
23	2000	114:00:00–115:08:24	15.83	0.62	0.11	0.004	0.28	0.007		3.9	0.001
24*	2000	122:04:05–122:23:54	15.52	0.57	0.08	0.006	2.00	0.080	m	4.8	0.001
25*	2000	144:19:12–145:21:36	15.54	0.48	0.08	0.003	1.09	0.024	m	5.8	0.000
26*	2000	145:21:36–146:23:46	16.74	0.54	0.24	0.006	2.05	0.048		3.9	0.000
27*	2000	156:13:00–156:22:48	16.04	0.57	0.28	0.010	1.21	0.036	s	4.0	0.001
28*	2000	175:19:12–177:00:00	14.58	0.50	0.02	0.002	0.53	0.012		6.0	0.000
29	2000	194:02:24–194:12:00	16.29	0.86	0.02	0.004	0.32	0.015		2.9	0.096
30	2000	222:00:00–222.18:00	15.24	2.28	0.09	0.008	0.46	0.031	s	0.2	0.476
31	2000	225:18:00–226:02:24	17.65	0.61	0.06	0.005	1.40	0.067	s	2.7	0.018
32	2000	235:00:00–236:23:45	16.72	0.89	0.39	0.020	1.09	0.070	m	1.7	0.466
33*	2000	272:00:00–273:23:46	15.09	0.54	0.07	0.004	0.56	0.014		5.6	0.000

NOTE.—Asterisks indicate those events with Fe charge states measured in the lowest energy range (0.062–0.11 MeV nucleon^{-1}), lowest energy included in ΔQ computation.

To select impulsive energetic particle events we used the following criteria. We started with all events that show $Q_{Fe} \geq 14$ in the SEPICA survey energy range of 0.18–0.43 MeV nucleon^{-1}, based on the observation that typical CME-related events and interplanetary shock events showed charge-state ranges from $Q =$ 10 to 12 when observed with *ACE* SEPICA in this energy range, with a few exceptions. This starting selection of 42 events may contain interplanetary shocks that are strongly enriched in Fe and ^{3}He as reported by Mason et al. (1999) and Desai et al. (2001). Therefore, we eliminated in a next step all events that are contained in the survey by Desai et al. (2003) and in the *ACE* shock list.[4] This step eliminated three events. To constrain our selection further we looked for evidence of a short time injection and time dispersion in the dynamic spectra of the events taken with *ACE* ULEIS, since such an injection signature has been identified as hallmark of impulsive events (Mazur et al. 2000a, 2000b). Such events are either marked with "s" for single injection or "m" for multiple injections (we have treated events with multiple injections within a few hours as one event) in Table 1. Twenty-four or about $\frac{2}{3}$ of the final number of events have this designation. As pointed out by Mazur et al. (2000a, 2000b), the impulsive events may be interrupted or only seen for a short time so that a number of events will be missed applying such a stringent criterion. Therefore, we made use of the observation that impulsive events that have been identified based on other observations have shown a substantial increase in Q_{Fe} with energy (Möbius et al. 2003) to expand our database. As can be seen in Table 1, all of the (admittedly few) events for which the charge state could also be obtained in the lowest energy range and that exhibit a clean injection signature show a strong increase in charge state over the entire energy range of more than 2.5 charge units, often much higher. A smaller increase of $\Delta Q = 1$–2 has also been observed in interplanetary shock events and interpreted as the result of rigidity-dependent escape from the acceleration region (Klecker et al. 2001), but a larger increase is not possible with this process. Consequently, we require ΔQ to be significantly different from zero for the Fe charge states as an alternate criterion. We use a student t-test with $p < 0.1$ and $\Delta Q > 2.5$ as selection criteria. For events without charge-state observation at the lowest energy this criterion may be too conservative, and some impulsive events may be eliminated from the survey. This criterion eliminated six additional events from the survey. With this combination of selection criteria, SEPICA charge-state data could be obtained for 33 impulsive events over three energy ranges: 0.18–0.25, 0.25–0.36, and 0.36–0.54 MeV nucleon^{-1}. Obtaining the charge states in the extended energy range (0.062–0.11 MeV nucleon^{-1})

[4] See http://www-ssg.sr.unh.edu/mag/ace/ACElists/obs_list.html.

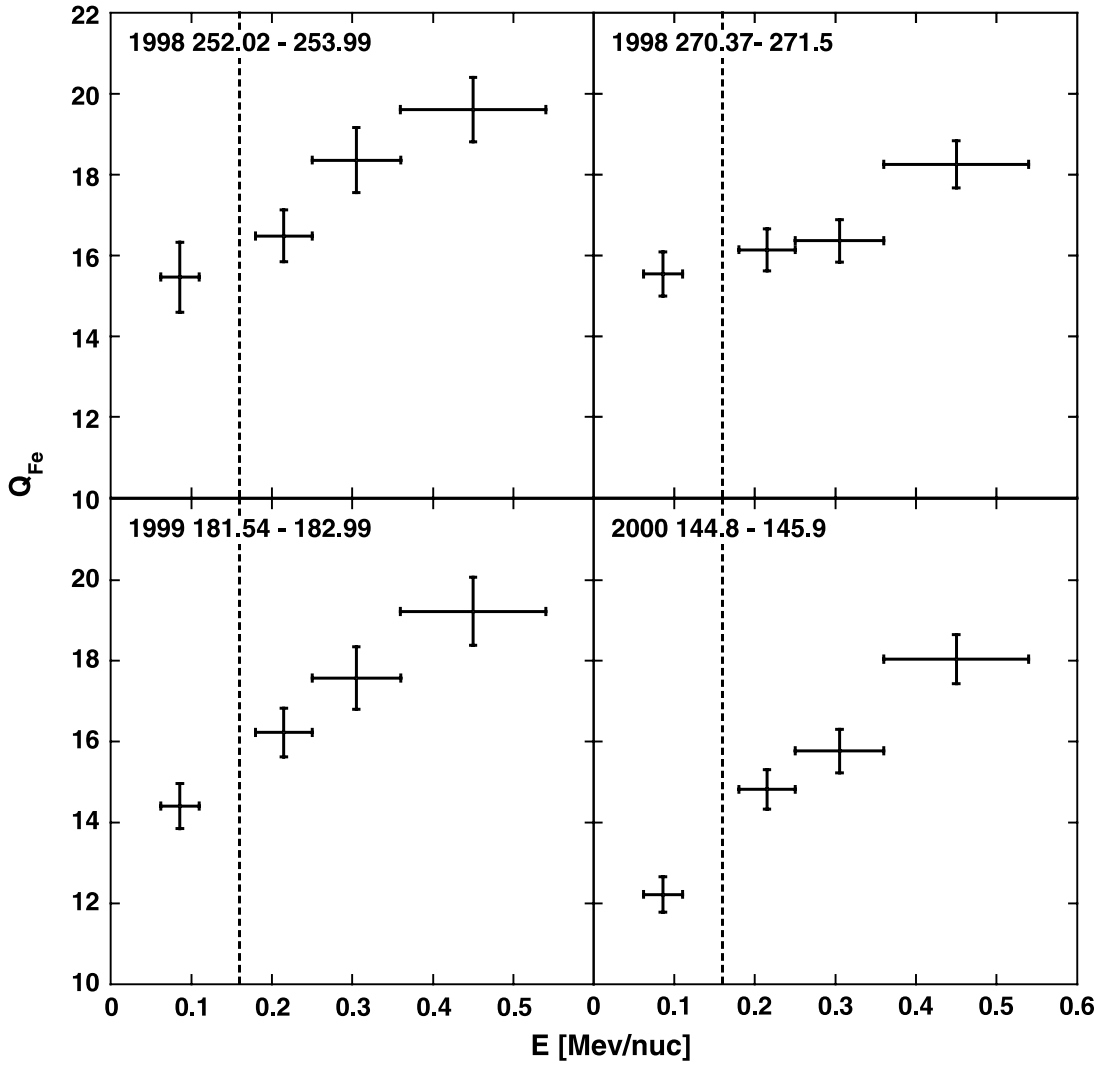

FIG. 2.—Fe charge states vs. energy (both linear) for four different impulsive events with good counting statistics. The error bars along the energy axis indicate the individual energy ranges, and the ones along the vertical axis show the statistical uncertainty of the mean charge states. The data point to the left of the dashed line has been taken from the extended energy range.

is more demanding. Due to poor statistics or lack of counts in the N track and/or the combined N-Fe range, charge states could only be obtained for 14 of the events in Table 1 at this energy range (noted with an asterisk at the event number). Three of the events in this category passed the $\Delta Q > 2.5$ criterion based only on the inclusion of the extended energy range (events 2, 10, and 33). However, these events passed the criterion by a large margin with $\Delta Q = 3.7$, 5.1, and 5.6, respectively.

3. RESULTS

In a first step the Fe charge states of the selected events will be determined for three different energy ranges or four, where possible. These energy-dependent charge states will then be compared with several ion abundance ratios.

3.1. *Energy-dependent Charge States*

Figure 2 shows the Fe charge states as a function of energy for four of the impulsive events with the best counting statistics, which minimizes the charge-state uncertainty. The horizontal error bars in the figure show the width of the energy range for each point. The three data points on the right represent the original energy range investigated by Möbius et al. (2003), and the point to the left of the dotted line is the new extended energy range. The gap in the data between 0.11 and 0.18 MeV nucleon^{-1} is due to overlap between the Fe track by Mg, Ne, and O (see Fig. 1), thereby precluding a measurement of Fe in this range.

All the impulsive events shown have Fe charge states that increase substantially with energy throughout the entire energy range. Even the event with the least variation (1998 DOY 270–271) shows an increase of 2.7 charge units from the lowest energy point of $Q \approx 15$, to $Q \approx 18$ at the highest energy. The event on 2000 DOY 144–145 shows the largest increase of six charge units, from $Q \approx 12$ to 18. At the lowest energy the charge states, which reach $Q \approx 12$–15, do not appear to flatten yet, probably indicating that the lowest charge state is not yet reached at these energies. Klecker et al. (2006) performed a similar study by combining the charge-state data from SEPICA with the data from CELIAS/STOF on *SOHO*. The STOF data extend in energy down to 0.01 MeV nucleon^{-1}. At these energies, Klecker et al. (2006) observed charge states ranging from 11 to 13. They concluded that their lowest points are consistent with a charge distribution in a $(1.2–1.8) \times 10^6$ K plasma. In the lowest SEPICA energy range we also obtained charge states of $\approx$11–13 for the event on 2000 DOY 144–145 (see Fig. 2) and for seven other events listed in Table 2.

TABLE 2
IMPULSIVE EVENTS FROM THIS STUDY WITH LOW-ENERGY CHARGE-STATE INFORMATION

EVENT NUMBER	YEAR	0.062–0.11 MeV nucleon $^{-1}$ (Q_{Fe1})	0.36–0.54 MeV nucleon $^{-1}$ (Q_{Fe4})	INFERRED QUANTITIES FROM LOW-ENERGY Q STATES			
				log T_{Pl}	Q_O	Q_{Ne}	Q_{Mg}
2	1998	15.24 ± 1.32	18.94 ± 0.99	6.44 ± 0.32	7.24 ± 0.69	8.18 ± 1.22	9.98 ± 0.43
9	1998	15.46 ± 0.87	19.61 ± 0.8	6.48 ± 0.24	7.43 ± 0.53	8.28 ± 0.99	9.99 ± 0.31
10	1998	12.51 ± 0.69	17.6 ± 0.63	6.24 ± 0.04	6.34 ± 0.13	8.00 ± 0.01	9.88 ± 0.04
11	1998	15.54 ± 0.55	18.25 ± 0.58	6.49 ± 0.18	7.50 ± 0.45	8.31 ± 0.72	9.99 ± 0.18
12	1999	13.39 ± 0.95	17.85 ± 1.38	6.29 ± 0.06	6.51 ± 0.30	8.01 ± 0.05	9.92 ± 0.05
13	1999	14.41 ± 0.56	19.22 ± 0.84	6.35 ± 0.04	6.84 ± 0.21	8.06 ± 0.04	9.95 ± 0.01
14	1999	12.37 ± 0.75	16.62 ± 1.06	6.23 ± 0.05	6.31 ± 0.14	7.99 ± 0.01	9.87 ± 0.08
15	1999	14.58 ± 0.79	18.32 ± 0.89	6.37 ± 0.09	6.90 ± 0.45	8.07 ± 0.17	9.96 ± 0.03
26	2000	13.11 ± 1.01	17.87 ± 0.74	6.27 ± 0.06	6.45 ± 0.28	8.01 ± 0.04	9.91 ± 0.05
27	2000	12.22 ± 0.44	18.04 ± 0.61	6.22 ± 0.03	6.29 ± 0.08	7.99 ± 0.01	9.86 ± 0.04
28	2000	14.2 ± 0.55	18.05 ± 0.68	6.34 ± 0.04	6.76 ± 0.20	8.05 ± 0.04	9.95 ± 0.01
29	2000	13.91 ± 0.79	17.87 ± 0.76	6.32 ± 0.06	6.65 ± 0.29	8.03 ± 0.05	9.94 ± 0.03
30	2000	10.81 ± 0.46	16.79 ± 0.76	6.12 ± 0.03	6.09 ± 0.11	7.97 ± 0.10	9.59 ± 0.19
35	2000	11 ± 0.53	16.56 ± 0.78	6.14 ± 0.04	6.12 ± 0.06	7.98 ± 0.01	9.64 ± 0.13

In Table 2 we have compiled the Fe charge states in the lowest and highest energy ranges for those 14 events in Table 1 (noted with asterisks) that allowed analysis in four energy ranges. As can be seen, half of these events exhibit a low-energy charge state $Q_{Fe1} < 13.5$. Assuming that these charge states are close to the thermal equilibrium state in the source plasma, we have deduced the corresponding plasma temperatures according to the tables by Arnaud & Raymond (1992). The log of the temperature is shown along with its uncertainty in column (5). Under these assumptions, the inferred temperatures range from 1.3 to 3×10^6 K. Table 2 also contains inferred charge states for O, Ne, and Mg according to the tables by Arnaud & Rothenflug (1985), which will be used later in the paper.

To test the statistical significance of the increase of Fe charge states with energy in our sample of impulsive events and to see whether our two selection criteria produce samples with a similar behavior, we have applied a linear fit to the charge-state increase using all events with a clear injection signature and all events with $\Delta Q > 2.5$ over the three highest energy ranges. To take out the substantial event-to-event variation in the average charge states and to just evaluate the increase with energy, we show the quantity $Q_{Fe}(E)$–Q_{mean} as a function of energy for all these events in the survey in Figure 3, where Q_{mean} is the mean charge state in the energy range 0.18–0.43 MeV nucleon^{-1} for each event. The left panel contains all events with a clear injection signature, and the right panel shows all events with $\Delta Q > 2.5$ over the upper three energy bands in our survey.

Although there is significant scatter in the increase of Q state with energy, both samples show a highly statistically significant increase between 0.2 and 0.45 MeV nucleon^{-1}. A statistical t-test returns values for $p < 10^{-6}$, leaving no doubt about the increase in all events in the survey. The fit parameters for the events with clear injection signature (Fig. 3, *left*) correspond to an average $\Delta Q = 2.7$ in the energy range 0.18–0.54 MeV nucleon^{-1}. This

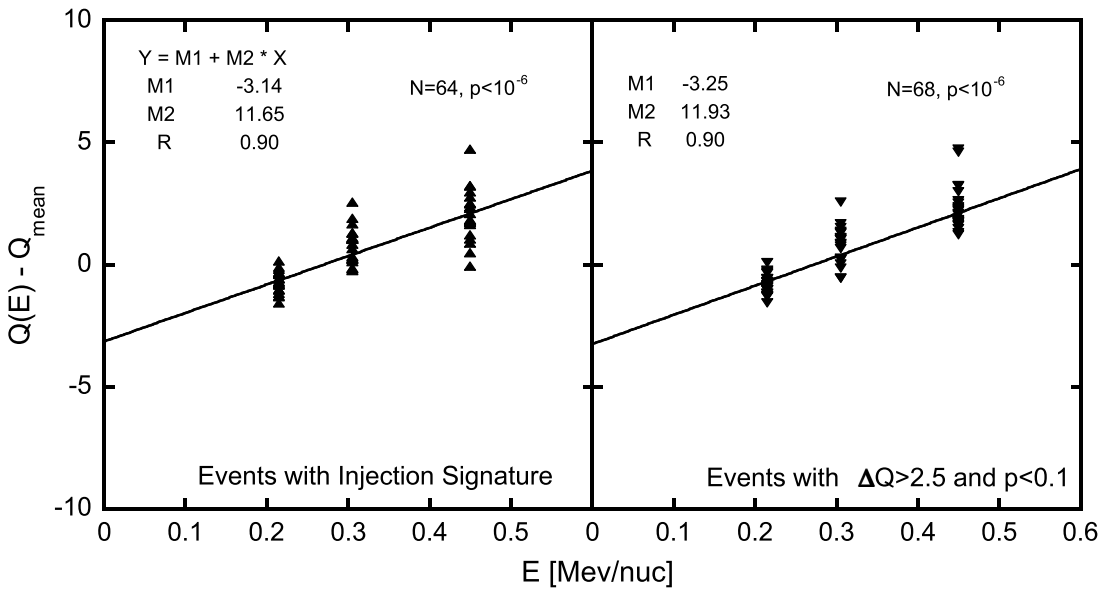

FIG. 3.—Fe Q states in the upper three energy bands, shifted by Q_{mean} for each event, as a function of energy (both linear) along with linear fits and the fit parameters. All events with a clear injection signature are shown on the left, and all events with $\Delta Q > 2.5$ over the three energy bands are on the right.

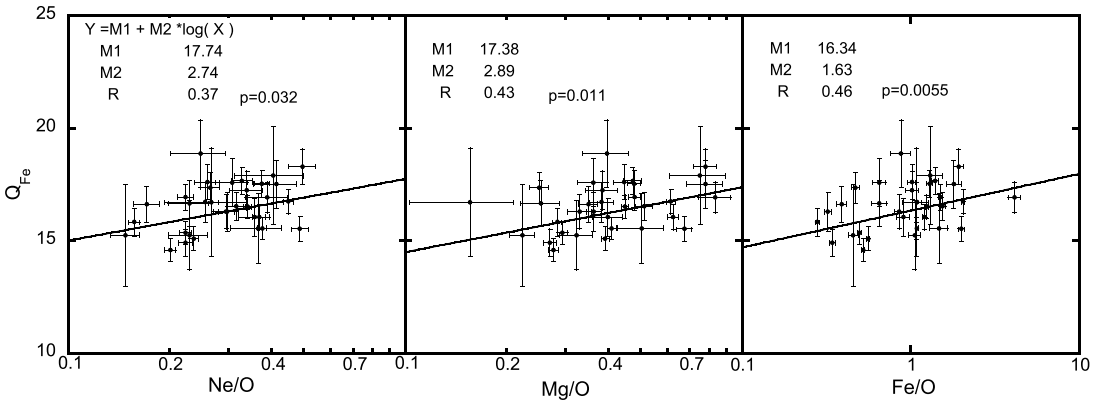

FIG. 4.—Fe charge states in the energy range 0.18–0.43 MeV nucleon^{-1} (linear) as a function of heavy ion abundance ratios at the center energy of 0.24 MeV nucleon^{-1} from *ACE* ULEIS (logarithmic). *Left*: Ne/O; *middle*: Mg/O; *right*: Fe/O. A logarithmic fit has been applied to each data set whose fit lines and parameters are included.

lends additional support for our alternate criterion, requiring a conservative $\Delta Q > 2.5$ for the inclusion of events not showing clear injection signatures.

3.2. *Dependence of the Ion Abundance on the Charge States*

In their survey of SEP events during the first year of the *ACE* mission, Möbius et al. (2000) found a positive correlation between the mean charge states of Fe and the abundances of heavy ions. Here we examine whether such a correlation persists between the abundance ratios and charge states when the selection is limited to impulsive events. Furthermore, the observed strong energy dependence of the charge states suggests that a correlation with the abundance ratios may also show a dependence on energy. In particular, the fact that the low-energy charge states appear to reflect the temperature in the source region (Klecker et al. 2006; Kartavykh et al. 2006) may point to a potential physical connection with abundance enhancements. To explore these possibilities, we first test the data set for a correlation between ion abundances and mean Fe charge states in the survey energy range and then repeat the analysis for the charge states separated into the four energy ranges shown in Figure 2, when available, or only the upper three for the remaining events.

Figure 4 shows the Fe charge states for the survey energy range as a function of Ne/O (*left panel*), Mg/O (*middle panel*), and Fe/O (*right panel*) taken at the energy of 0.24 MeV nucleon^{-1} with *ACE* ULEIS. Each data point shows the mean charge state and the abundance ratio for one impulsive event with the respective uncertainties for all 33 events in Table 1. Because the abundance ratios vary by up to almost 2 orders of magnitude for Fe/O and charge states are confined to a limited range, abundance ratios are shown on a logarithmic scale while a linear scale is chosen for the charge states.

While the correlation coefficient R reaches only moderate values of $\sim$0.4, the statistical t-test returns p-values of 0.034, 0.021, and 0.046; i.e., the observed positive correlation of charge state with each of the three abundance ratios shows a probability of arising by chance of $<5\%$ in all three cases. It should be pointed out that the probability of arising by chance is consistently low for all three heavy ion species, which reemphasizes the observed correlation. No correlation is found with the ^{3}He/^{4}He ratio in a similar analysis, for which the corresponding p-value is 0.35.

Figure 5 shows the Fe charge states (separately for the four energy ranges used in Fig. 2) as a function of the Fe/O abundance ratio. When the charge-state information is split up according to energy ranges, all 33 impulsive events from Table 1 can be used in the upper three energy ranges between 0.18 and 0.54 MeV nucleon^{-1}, but only the 14 events in Table 2 could be analyzed in the extended energy range (0.062–0.11 MeV nucleon^{-1}). Therefore, only these 14 events are shown in the upper left panel, while all events are plotted for the upper three energy ranges, increasing in energy, from the upper right to the lower right panel. The straight lines indicate the logarithmic least-squares fit regression curves, for which the fit parameters are shown in the upper left corner of each panel.

A noticeable trend of the Fe charge states with the Fe/O ratio appears to be visible to varying degree in all plots, except for the highest energy range (0.36–0.54 MeV nucleon^{-1}). Here the charge states do not show any dependence on the Fe/O ratio, and the scatter in the data points is most prevalent. The Mg/O and Ne/O ratios (not shown) behave similarly to Fe/O, but with some more scatter. A similar analysis for the ^{3}He/^{4}He ratios (not shown) does not show any trend, except for the lowest energy range with only 14 events.

Figure 5 also shows logarithmic fits of the Fe charge states as a function of the Fe/O ratio (linear in the semilogarithmic representation of the plot). To evaluate the trends visible in the Fe/O quantitatively for all species, the slopes, the correlation coefficients R, and the resulting p-values from the statistical t-test are compiled in Table 3 for all four energy ranges of the charge states. For the lowest energy range the entries are based on the 14 events in Table 2 for which the analysis in the extended energy range is possible. The remaining three energy ranges contain information from all events in Table 1. In each individual energy range a few events had to be omitted for lack of statistics. The number of events included is given in the last column.

While the slopes of the fit turn out positive for all combinations of abundance ratios and Q states, the values of the slopes are generally very low for the He isotope ratio and for heavy ions in the highest energy range. The correlation coefficients are generally moderate near 0.4 for the heavy ion ratios, except for the highest energy range (0.36–0.54 MeV nucleon^{-1}), where they are very low (<0.2) for all species. The helium isotope ratio has a low correlation coefficient except for the lowest energy range. More telling are the results from the t-test. If we set 5% as a threshold below which the p-value should fall to indicate a statistically significant correlation, i.e., the probability that a correlation occurs by chance is below 5%, the results in Table 3 exclude the highest and lowest energy ranges as well as all He isotope ratios from consideration. Because the p-values are reduced for larger samples with a similar trend, the higher p-values for the lowest energy range may be due to the limited number of events, and the test is inconclusive. However, the heavy ion ratios

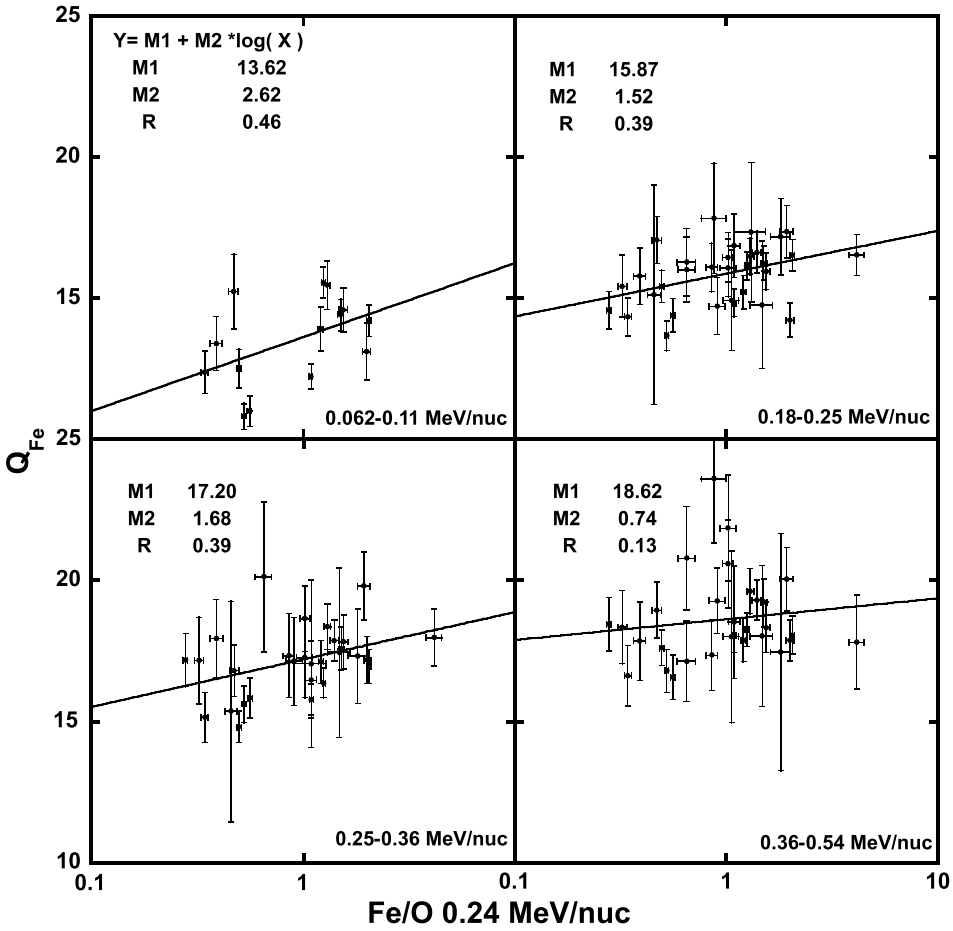

FIG. 5.—Fe charge states on a linear scale in four different energy ranges as a function of Fe/O at 0.24 MeV nucleon^{-1} on a logarithmic scale. Selection of impulsive events from 1997 to 2000 presented in Table 1. The lowest energy range contains only the 14 events in Table 2, while the other three energy ranges contain all events in Table 1. The lines obtained in a least-squares fit are also shown.

pass a 5% test in two of three cases for 0.18–0.25 and 0.25–0.36 MeV nucleon^{-1}, while the values reach or exceed 50% for all species at 0.36–0.54 MeV nucleon^{-1} and are rather high throughout for the ^{3}He/^{4}He ratio.

Summarizing, we find a consistent correlation between the heavy ion abundance ratios and the Fe charge state except for the highest energy range. We note that the statistical significance of the heavy ion correlation at the lowest energy is limited due to the small number of events. There appears to be no correlation with the ^{3}He/^{4}He ratio.

4. DISCUSSION

In this work, we have extended our earlier work (Möbius et al. 2003; Klecker et al. 2006) on the energy dependence of ionic charge states in impulsive events by surveying more events and measuring charge states to lower energies. The data show that the Fe charge states consistently depend on the energy throughout the entire energy range covered by SEPICA for the entire set of 33 impulsive events studied here. The charge states show a strong increase with energy of up to six charge states with no clear indication for a leveling off in the lowest energy range of the SEPICA instrument. For 14 of these events the charge-state measurement could be extended to energies between 0.06 and 0.11 MeV nucleon^{-1}. Here the Fe charge states fall between $\approx$11 and $\approx$15; i.e., they are much lower than previously thought as typical for impulsive events.

The strong energy dependence of the Fe charge states in impulsive events found in earlier, more limited, event studies has been confirmed statistically in this survey of events with *ACE*. The observed variation of the charge states with energy is consistent with models by Kartavykh et al. (2006, 2007) that are based on acceleration out of a source plasma with temperatures between 1.3 and 3 million K and stripping during acceleration of the ions to higher energies, which leads to the observed increase of charge state with energy (see also Klecker et al. 2006). No alternative to this explanation is known at present for the observed strong increase of charge state with energy at $E < 1$ MeV nucleon^{-1}. It should be noted that a reverse stripping process, i.e., the acceleration of ions out of a high-temperature source region, followed by recombination and stripping during the traversal of a low-temperature plasma into an energy-dependent charge-state distribution as observed, is highly improbable because the timescales for recombination are substantially longer than those for stripping, as has been shown by Kocharov et al. (2000) and Kartavykh et al. (2008). As a consequence, our findings lend strong support to the conclusion that ions in impulsive events must be accelerated at low altitudes in the corona. The inferred stripping requires values of $Nt_{\rm acc} \sim 10^{10}$–$10^{11}$ s cm^{-3}, where N is the density and $t_{\rm acc}$ is the acceleration timescale (see Kartavykh et al. 2006). Thus, acceleration timescales in the range of $\sim$1–10^3 s would require densities in the range of 10^7–10^{11} cm^{-3}, i.e., altitudes of $<0.5\,R_S$ above the photosphere.

As a second important point, it is evident that the inferred source temperatures for the 14 events that allow a low-energy charge analysis fall below the temperature range of 3–5 million K, inferred from abundance measurements in impulsive events by

TABLE 3
PARAMETERS FOR FITS OF ABUNDANCE RATIOS VS. Fe Q STATES OVER FOUR DIFFERENT ENERGY RANGES

Parameter	^{3}He/^{4}He 0.39 MeV nucleon^{-1}	Ne/O 0.24 MeV nucleon^{-1}	Mg/O 0.24 MeV nucleon^{-1}	Fe/O 0.24 MeV nucleon^{-1}
Energy Range for Q_{Fe}: 0.062–0.11 MeV nucleon^{-1}; 14 Events				
Slope	1.80	4.25	3.71	2.62
R	0.48	0.39	0.34	0.46
p	0.081	0.17	0.24	0.098
Energy Range for Q_{Fe}: 0.18–0.25 MeV nucleon^{-1}; 32 Events				
Slope	0.19	2.36	2.55	1.52
R	0.15	0.31	0.38	0.39
p	0.44	0.087	0.032	0.025
Energy Range for Q_{Fe}: 0.25–0.36 MeV nucleon^{-1}; 29 Events				
Slope	0.43	3.59	3.24	1.68
R	0.26	0.41	0.45	0.39
p	0.18	0.027	0.013	0.035
Energy Range for Q_{Fe}: 0.36–0.54 MeV nucleon^{-1}; 30 Events				
Slope	0.11	1.54	1.07	0.74
R	0.05	0.13	0.10	0.13
p	0.79	0.51	0.60	0.50

NOTE.—14 events from Table 2 are in the first set of rows, and 33 events from Table 1 are in the remaining rows. Slope and correlation coefficients (R) are from a logarithmic fit; p-values are from t-test.

Reames et al. (1994). It should be pointed out that the Fe charge-state observations at 0.06–0.11 MeV nucleon^{-1} probably even provide an upper limit to the temperature, because in the case when *SOHO* STOF observations at even lower energy are available, that charge state falls even below the value obtained at the lowest SEPICA energy (Klecker et al. 2006). It should be noted that the results presented here represent a more direct determination of the source temperature necessary for the explanation of the data than inference from ion abundances.

The low source temperatures for the energetic ions may also be contrasted with observations of EUV jets in the inferred source regions of ^{3}He-rich events by Pick et al. (2006). Models for such jets observed in solar flares place their temperature at $(3–8) \times 10^6$ K (Shimojo & Shibata 2000), much higher than the temperatures indicated by the observed Fe charge states. This obvious substantial difference may point to a separation in space and/or time of the exact location of the jets and the source region for the energetic particles, but at this point these differences remain unresolved.

In the second part of this paper we have investigated whether there is a significant correlation between the observed Fe charge states and abundance ratios in the impulsive events and whether there is energy dependence in such a correlation. From the observation reported here, a significant correlation between the mean Fe charge state in the events and abundance ratios of heavy ions have been found, while no clear correlation for the ^{3}He/^{4}He ratio is found. The behavior of the He isotopes may be consistent with findings that the ^{3}He/^{4}He ratio generally does not correlate well with the heavy ion abundances except for ^{3}He/^{4}He ratios smaller than 0.1 (e.g., Dwyer et al. 2001). Our full sample contains several events with extremely high ^{3}He/^{4}He ratios, which do not show a further increase in charge state and thus tend to erase any correlation.

When separating the charge-state data by energy, a clear trend for a change of the correlation between abundance ratios and charge state with energy emerges, at least for the three energy ranges with the full complement of events. While there is a significant correlation with a rather low probability of chance involvement for 0.18–0.36 MeV nucleon^{-1}, the correlation disappears at the highest energy. This behavior appears to be consistent with the model for the observed strong energy dependence of the charge states. Because the model connects the low-energy charge states to the source temperature, it would suggest a correlation of the abundance ratios with charge state at low energies, since all known models to explain abundance enhancements rely on mass per charge ratio differences at injection and/or during acceleration. Unfortunately, the results at the lowest energy, which should show this behavior most clearly but where only 14 events can be used, are statistically inconclusive. Conversely, the charge state at high energies is solely determined by stripping according to ion energy, which leads to fixed mass per charge ratios for any given energy and cannot produce event-to-event variations in selective acceleration. This expected trend agrees well with the observed disappearance of the correlation at the highest energies.

Still, the direction of the observed correlation is the opposite of what one might naively expect. Generally, the abundance enhancements increase for higher charge states; i.e., they become larger as the ions progress toward a fully stripped state. If the ion abundance enhancement mechanism operates on different Q/M ratios, then why would the enhancements become larger as the Q/M ratios approach a common limit of 0.5?

In order to search for other possible trends in the Q/M ratios of the elements in our survey, it would be useful to examine Q/M for O, Ne, and Mg at the same low energy where Fe Q states correlate with the abundance enhancements. Since SEPICA determines charge states for these ions only at significantly higher energies than necessary to reflect conditions before significant stripping occurs, we estimated these charge states by assuming charge equilibrium for all species according to the plasma temperature at the acceleration site. This plasma temperature was estimated using the observed Fe Q state in the lowest energy range of SEPICA (0.062–0.11 MeV nucleon^{-1}) given in Table 2, together with the tables of equilibrium charge states by Arnaud

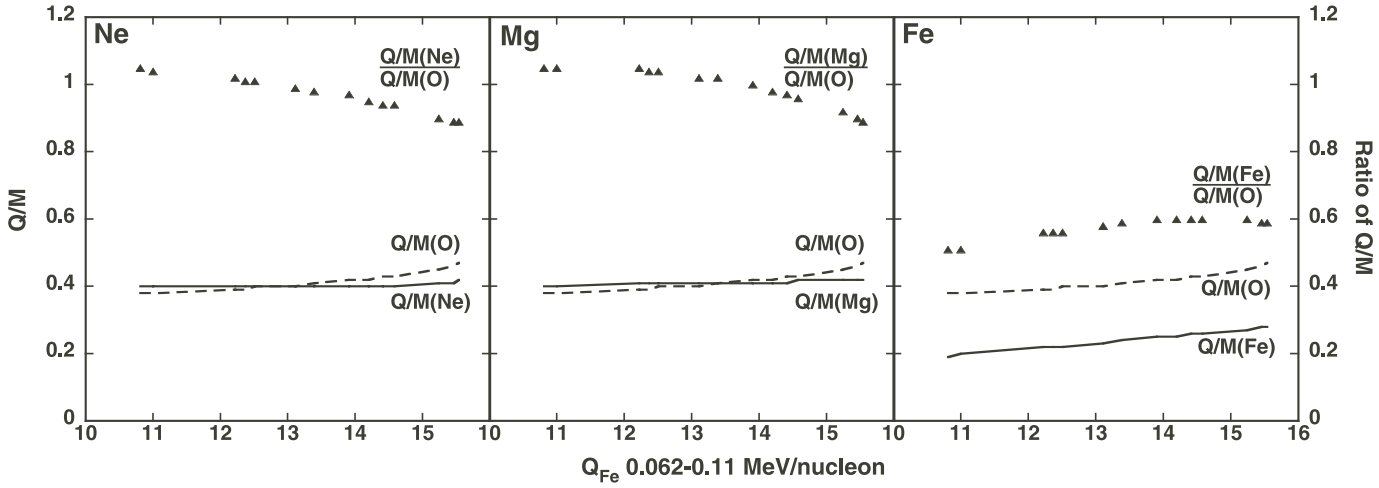

FIG. 6.—Q/M ratios for O, Ne, Mg, and Fe as inferred from the Fe Q states in the lowest energy range assuming ionization equilibrium according to Arnaud & Rothenflug (1985) and Arnaud & Raymond (1992) as a function of Fe Q states. The Q/M ratios for Ne and O and the respective ratio for Ne over O are shown in the left panel. The same information is shown for Mg in the middle panel and for Fe in the right panel, all ratios based on O.

& Raymond (1992). We note that our inferred Fe temperatures should be treated as upper limits, since the *SOHO* STOF instrument has observed Fe Q states even lower than our lowest values. However, this simple analysis should allow us to probe the direction of trends in the observations and the models. Given the plasma temperatures for each of the 14 events with low-energy Fe Q states, we then calculated the mean charge states of O, Ne, and Mg (also given in Table 2), using the tables by Arnaud & Rothenflug (1985). For the species used here the charge-state fractions and mean charge states as a function of temperature compiled by Arnaud & Rothenflug (1985) and Arnaud & Raymond (1992) agree with the more recent compilation by Mazzotta et al. (1998) to much better than 1%. Both groups have included the same set of physical effects in their modeling. Using the measured Q states of Fe at 0.062–0.11 MeV nucleon^{-1} and the inferred Q states of O, Ne, and Mg as described above, Figure 6 shows (*from left to right*) the resulting Q/M ratios along with the ratios of Q/M for Ne ($M = 20$), Mg ($M = 24$), and Fe ($M = 56$) over that of O ($M = 16$) as a function of the observed Fe Q state in the 14 impulsive events.

Surprisingly, the Q/M ratios of Ne and Mg show almost no increase as a function the observed Fe Q state (see also Reames et al. 1994, their Fig. 14). Only the Q/M ratios of O and Fe show noticeable increases, O by about 25%, and Fe by about 50% over the observed range. As can be seen in Figure 6, these variations conspire to positive trend for the ratio of the Q/M values of Fe over O, but to a negative trend for the respective ratios for Ne and Mg as a function Q_{Fe}. In addition, both the Ne and Mg Q/M values cross that of O for Fe Q states close to 13. The Ne and Mg behavior obviously arises from the fact that the Q states of Ne and Mg do not vary significantly in the temperature range between 1 and 3×10^6 K, inferred from the Fe Q-state observations, while the Q state of O does change. Because Q/M is thought to be the main control parameter for selective acceleration, these results are puzzling. Ne and Mg are clearly enhanced over O along with Fe, which always shows the strongest effect, not counting ultraheavy ions, and the abundances relative to O of these species exhibit a similar positive correlation with the Fe Q state. Yet compared with O, the Q/M values show opposite trends for Ne and Mg on one side and Fe on the other side.

In order to discuss these results in light of current models for selective acceleration, let us take a brief look at predictions from those models that employ resonant wave particle interactions. The model by Miller & Vinas (1993; see also Miller et al. 1993a, 1993b; Miller 1998), uses shear Alfvén waves to enhance the heavy ions. Assuming a plasma at 3×10^6 K, Miller (1998) demonstrates that the cyclotron frequencies of Ne, Mg, and Fe lie in a range where these Alfvén waves are excited, while those of C, N, and O lie outside this range and thus will not be accelerated by these waves. The main difference between these two groups of species is that, at 3×10^6 K, Q/M for C, N, and O is relatively close to 0.5, while the Q/M value for Ne, Mg, and Fe is considerably lower. Because the cyclotron frequency of Fe (with the lowest Q/M) lies close to the waves with the highest growth rate, it will undergo an even stronger acceleration than Mg and Ne. As the charge states of the heavy ions increase and Q/M moves closer to 0.5, their cyclotron frequencies shift to regions with a lower growth rate. As a result, a negative correlation between the abundance ratios and Q/M ratios, and thus Fe charge states would be expected from this model.

The model by Temerin & Roth (1992) also predicts a negative correlation between the abundance ratios and charge states. Temerin & Roth (1992) use electromagnetic ion cyclotron waves to describe the ion enhancements. Their model suggests that ions with a Q/M near 0.5 will not be preferentially heated, while ions with Q/M below 0.5 will be preferentially accelerated. Thus, the ions with higher charge states should show a smaller enhancement, opposite to what is observed.

Models that invoke rigidity-dependent acceleration and escape from the acceleration region, such as those discussed by Möbius et al. (1982) and by Ellison & Ramaty (1984), appear to qualitatively agree with the results in this study. These models predict enhancements that are dependent on the rigidity of the ions, which is proportional to M/Q. As the rigidity of the ions decreases, the escape from the magnetic fields in the acceleration region becomes less efficient, and the ions can be accelerated for a longer time. Therefore, as the ionic charge state increases, the ions will escape more slowly, thus resulting in an enhancement of heavy ions. However, this explanation would only hold for Fe, because Fe is the only species that shows a decrease of the M/Q ratio compared to O as a function of the Fe Q state (which correlates with the abundance ratios). In addition, the rigidity-dependent models predict significant enhancements of selected species only at higher energies, because only there is escape from the acceleration region possible. However, no correlation between charge states and abundance ratios is observed at these energies.

In summary, none of the selective acceleration models seems to agree with the observed correlation between abundance ratios and charge states particularly at low energies. While these observations appear to be consistent in general with a mass per charge-dependent selection mechanism at the low energies where the injection occurs and subsequent stripping, quantitative predictions of these disagree with the observed trends. It appears that some additional feature would be required to explain these results. As a speculative example, it could be argued that the degree of Fe/O enhancement is related to the coronal height of the acceleration event. Such a behavior might be caused by gravitational settling, as, for example, discussed for Fe-rich events by Gloeckler et al. (1975). In that case, high Fe/O events would originate at lower coronal heights and would therefore also show more stripping. That could yield correlations of the type we see.

5. CONCLUSION

In a survey of a large sample of impulsive energetic particle events we have found a consistently strong energy dependence of the ionic charge state of Fe, which is in full agreement with previous observations and models that attempt to explain this behavior in terms of charge stripping during or after the acceleration out of a source with a temperature of $(1–3) \times 10^6$ K. This observation lends further support to the idea that the particle acceleration in these impulsive events occurs at low altitudes in the solar corona, i.e., at $<0.5\ R_S$ above the photosphere. The inferred source temperatures in impulsive events are substantially lower than those deduced previously from the observed ion abundance ratios and heuristic enhancement models.

Using the SEPICA charge-state data and ULEIS ion abundances, we have shown that there is a significant correlation between the abundance ratios of heavy ions and the Fe charge states for impulsive events. When splitting the charge state information according to energy, the correlation is seen for the lower two energy ranges that can be obtained for all impulsive events, but it disappears at the highest energy. Such a behavior is expected for charge states that are determined at low ion energies by the temperature of the source plasma and by stripping as a function of ion energy at higher energies. As a consequence, an even closer correlation would be expected for the extension to even lower energies. However, the limitation to less than half of the events for this analysis apparently compromises the statistical significance, and the results in this energy range are inconclusive. Therefore, charge-state observations that are better optimized to the low-energy range and extended over longer time will be needed to address the open questions left here.

In light of selective acceleration models based on resonant wave-particle interaction, the direction of the observed correlation of ion abundance with charge state seems to produce contradictory results. It remains puzzling and an unresolved problem that the charge states tend to change toward the fully stripped condition with increasing enhancements.

The authors are grateful to many dedicated individuals at UNH, UMD, APL, at the MPE, and at TUB for their enthusiastic contributions to the completion of the *ACE* SEPICA and ULEIS instruments. The work was supported at the University of New Hampshire, the University of Maryland, and at the Applied Physics Laboratory by NASA under grant NAG 5-12929 through subcontracts from the California Institute of Technology, and at Johns Hopkins University/Applied Physics Laboratory under NASA grant NNG04GJ51G.

APPENDIX

ANALYSIS METHOD TO EXTEND Fe CHARGE-STATE MEASUREMENTS WITH SEPICA TO LOW ENERGIES

Thus far charge states have been obtained with SEPICA over an energy range that is limited at low energies by the capability of the ΔE versus E detector system to clearly separate species. Figure 1 in the main section of the paper shows the separation of species in a ΔE versus E representation, where the Fe track crosses over those of the other species at energies below 0.18 MeV nucleon^{-1}. Below the strong O track Fe can be clearly distinguished again from the other species. In two energy ranges Fe is found with little competition: below the C track and where Fe intersects N between C and O (at 0.062–0.11 MeV nucleon^{-1}), because N is a minor species. In particular, in impulsive events with their heavy ion enhancement, the Fe track is very prominent at these low energies.

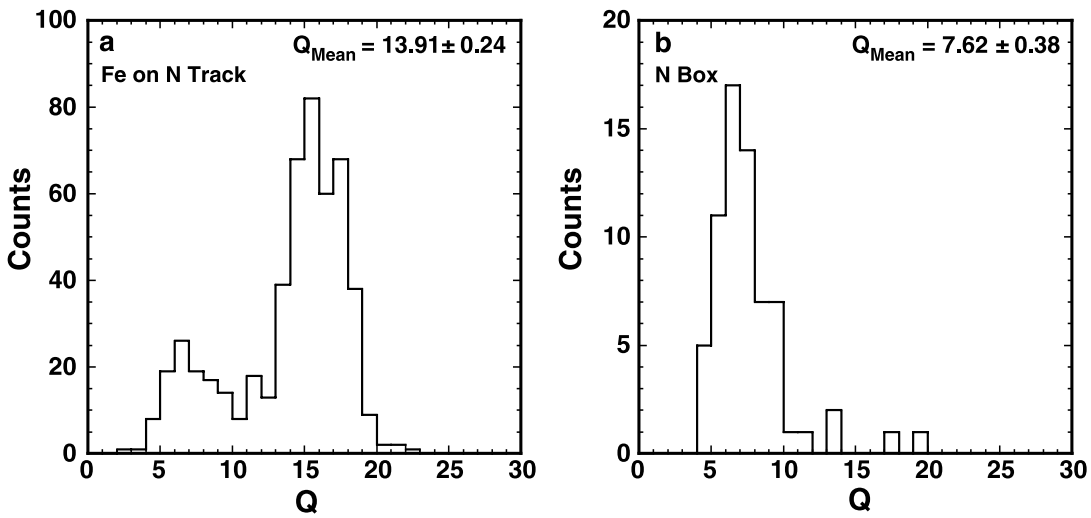

FIG. 7.—(*a*) Charge distribution of Fe and N in the overlapping region for the 1998 DOY 270.375–271.5 event. (*b*) Charge distribution of N in the energy range just above the overlapping region where N is clearly separated.

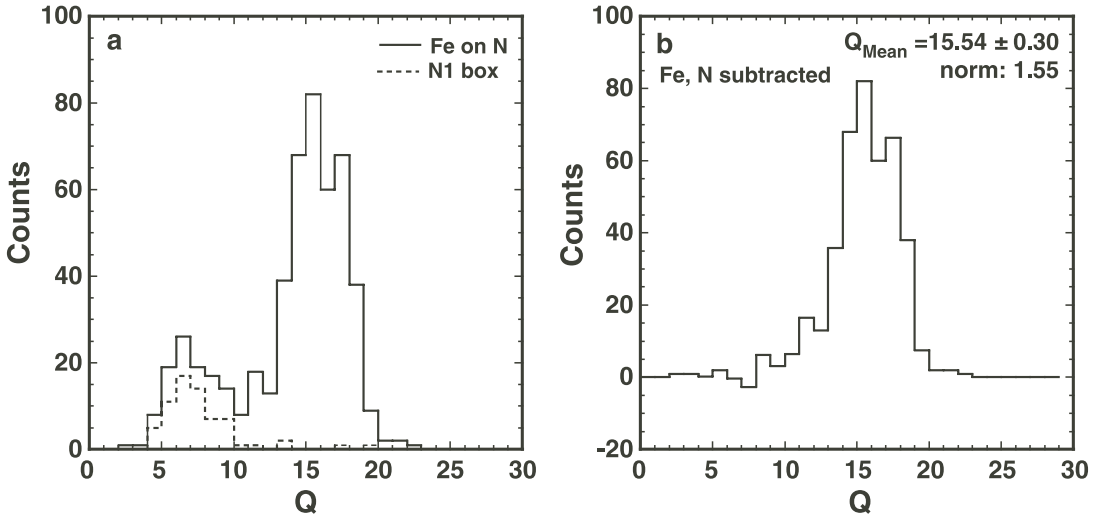

FIG. 8.—(*a*) Combined Fe and N distribution in the overlapping region for the event on 1998 DOY 270.375–271.5, overlaid (*dashed line*) with the N distribution from Fig. 7*b*. (*b*) Fe distribution in the overlapping region after subtracting the N counts, normalized to the extrapolated N flux and optimized for full N charge distribution subtraction at $Q = 5$–6.

Although we can reasonably assume that Fe is the only species below C, it turns out that at such low energies (<0.05 MeV nucleon^{-1}) part of the ions are deflected beyond the edge of the detector. Therefore, Fe in this region is not considered for this paper, which instead concentrates on the range between C and O. Obtaining an accurate measurement of the Fe charge states requires two steps in addition to the Fe charge-state computation based on electrostatic deflection and total energy of the ions, i.e., an estimate of the amount of N in the selected box and subtracting the N charge-state distribution as obtained from the clearly separated N at higher energies. As can be seen in Figure 7 for the event on 1998 DOY 270.375–271.5, the raw charge-state distribution as obtained in the overlapping energy range (Fig. 7*a*) indeed appears to have two components, one that represents Fe and one that represents N. The latter is evident from the N charge distribution taken in the energy range, where N is clearly separated (Fig. 7*b*). It should be noted that both distributions are obtained using a total energy based on Fe values for the energy loss in the proportional counter windows and the pulse height defect in the solid state detector.

To estimate the N counts, we extrapolate the N flux into the overlapping Fe and N ranges using the energy spectra obtained for the energy range with clear species identification. Because spectra tend to roll over, we generally use the two lowest energy points for the extrapolation. For use in the subtraction the flux is then converted back to the expected number of N counts, taking into account the geometric factor, accumulation time, and dead-time corrections for limited pulse height transmission in the telemetry. The latter corrections are usually rather small for impulsive events.

Figure 8 illustrates the subtraction process in the Fe charge-state determination. The combined charge-state distribution is repeated in Figure 8*a*, together with the N distribution from Figure 7*b* (*dashed lines*), before normalization to the extrapolated flux. Based on the total number of N counts in the overlapping range from the energy spectra extrapolation, the N distribution is to be renormalized for proper elimination of the N contamination in the Fe charge distribution. Because the normalization factor is obtained in a first step from a linear extrapolation of the observed energy spectra, often an over- or undercompensation for N counts may result. Therefore, the normalization factor is optimized in a second step such that the deviation from a zero baseline in the charge state range of N is minimized. The final Fe charge distribution, after subtraction of N with an optimized normalization factor (of ≈ 1.5 for the example), is shown in Figure 8*b*.

REFERENCES

Arnaud, M., & Raymond, J. 1992, ApJ, 398, 394
Arnaud, M., & Rothenflug, R. 1985, A&AS, 60, 425
Barghouty, A. F., & Mewaldt, R. A. 1999, ApJ, 520, L127
Desai, M. I., et al. 2001, ApJ, 553, L89
———. 2003, ApJ, 588, 1149
Dietrich, W. F. 1973, ApJ, 180, 955
Dwyer, J. R., et al. 2001, ApJ, 563, 403
Ellison, D. C., & Ramaty, R. 1984, Adv. Space Res., 4, 137
Fisk, L. A. 1978, ApJ, 224, 1048
Garrard, T. L., Stone, E. C., & Vogt, R. E. 1973, in High Energy Phenomena on the Sun, ed. R. Ramaty & R. G. Stone (NASA SP-342; Washington, DC: NASA), 341
Gloeckler, G., Hovestadt, D., Vollmer, O., & Fan, C. Y. 1975, ApJ, 200, L45
Hsieh, K. C., & Simpson, J. A. 1970, ApJ, 162, L191
Ibragimov, I. A., & Kocharov, G. E. 1978, in Proc. 15th Int. Cosmic Ray Conf. International Cosmic Ray Conference (Plovdiv), 221
Kahler, S. W. 1977, ApJ, 214, 891
Kartavykh, Y. Y., Dröge, W. Klecker, B., Kocharov, L., Kovaltsov, G. A., & Möbius, E. 2008, ApJ, 681, 1653
Kartavykh, Y. Y., Dröge, W. Klecker, B., Mason, G. M., Möbius, E., Popecki, M., & Krucker, S. 2007, ApJ, 671, 947
Kartavykh, Y. Y., Dröge, W., Kovaltsov, G. A., & Ostryakov, V. M. 2006, Adv. Space Res., 38, 516, DOI:10.1016/j.asr.2005.01.077
Klecker, B., Möbius, E., Popecki, M. A., Lee, M. A., & Bogdanov, A. T. 2001, in AIP Conf. Proc. 598, Solar and Galactic Composition, ed. R. F. Wimmer-Schweingruber (New York: AIP), 317
Klecker, B., et al. 1984, ApJ, 281, 458
———. 2006, Adv. Space Res., 38, 493, DOI:10.1016/j.asr.2005.04.042.
Kocharov, L., Kovaltsov, G. A., Torsti, J., & Ostryakov, V. M. 2000, A&A, 357, 716
Kovaltsov, G. A., Barghouty, A. F., Kocharov, L., Ostryakov, V. M., & Torsti, J. 2001, A&A, 375, 1075
Leske, R. A., et al. 2003, in AIP Conf. Proc. 679, Solar Wind Ten, ed. M. Velli, R. Bruno, & F. Malara (New York: AIP), 616
Liu, S., Petrosian, V., & Mason, G. M. 2006, ApJ, 636, 462
Luhn, A., Klecker, B., Hovestadt, D., & Möbius, E. 1987, ApJ, 317, 951
Mason, G. M., Mazur, J. E., & Dwyer, J. R. 1999, ApJ, 525, L133
———. 2002, ApJ, 565, L51
Mason, G. M., Mazur, J. E., & Hamilton, D. C. 1994, ApJ, 425, 843
Mason, G. M., Reames, D. V., von Rosenvinge, T. T., Klecker, B., & Hovestadt, D. 1986, ApJ, 303, 849
Mason, G. M., et al. 1998, Space Sci. Rev., 86, 409

Mason, G. M., et al. 2004, ApJ, 606, 555
Mazur, J. E., et al. 2000a, ApJ, 532, L79
———. 2000b, in AIP Conf. Proc. 528, Acceleration and Transport of Energetic Particles Observed in the Heliosphere, ed. R. A. Mewaldt et al. (New York: AIP), 47
Mazzotta, P., Mazzitelli, G., Colafrancesco, S., & Vittorio, N. 1998, A&AS, 133, 403
Miller, J. A. 1998, Space Sci. Rev., 86, 79
Miller, J. A., & Vinas, A. F. 1993, ApJ, 412, 386
Miller, J. A., et al. 1993a, in Proc. 23rd Int. Cosmic Ray Conf. (Calgary), 13
———. 1993b, in Proc. 23rd Int. Cosmic Ray Conf. (Calgary), 17
Möbius, E., Scholer, M., Hovestadt, D., Klecker, B., & Gloeckler, G. 1982, ApJ, 259, 397
Möbius, E., et al. 1998, Space Sci. Rev., 86, 449
———. 2000, in AIP Conf Proc. 528, Acceleration and Transport of Energetic Particles Observed in the Heliosphere, ed. R. A. Mewaldt et al. (New York: AIP), 131
———. 2002, Adv. Space Sci., 29, 1501
Möbius, E., et al. 2003, in Proc. 28th Int. Cosmic Ray Conf. (Tsukuba), 3273
Pick, M., Mason, G. M., Wang, Y.-M., Tan, C., & Wang, L. 2006, ApJ, 648, 1247
Reames, D. V. 1990, ApJS, 73, 235
———. 2000, ApJ, 540, L111
Reames, D. V., Dennis, B. R., Stone, R. G., & Lin, R. P. 1988, ApJ, 327, 998
Reames, D. V., Meyer, J. P., & von Rosenvinge, T. T. 1994, ApJS, 90, 649
Reames, D. V., & Ng, C. K. 2004, ApJ, 610, 510
Reames, D. V., Ng, C. K., & Tylka, A. J. 1999, Geophys. Res. Lett., 26, 3585
Sheeley, N. R., Jr., et al. 1975, Sol. Phys., 45, 377
———. 1983, ApJ, 272, 349
Shimojo, M., & Shibata, K. 2000, ApJ, 542, 1100
Stone, E. C., et al. 1998, Space Sci. Rev., 86, 1
Stovpyuk, M. F., & Ostryakov, V. M. 2001, Sol. Phys., 198, 163
Temerin, M., & Roth, I. 1992, ApJ, 391, L105
Varvoglis, H., & Papadopoulos, K. 1983, ApJ, 270, L95
Zhang, T. X. 1995, ApJ, 449, 916
Zhang, T. X., & Wang, J. X. 2003, ApJ, 588, L57